Resonances determination in microstructured films embedded in multilayered stacks

Benjamin Vial[a,b], Mireille Commandré[a], Frédéric Zolla[a], André Nicolet[a] and Stéphane Tisserand[b]

[a]Institut Fresnel, Université Aix-Marseille III, École Centrale de Marseille, France;
[b]Silios Technologies, France

ABSTRACT

Our approach consists in finding the eigenmodes and the complex eigenfrequencies of structures using a finite element method (FEM), that allows us to study mono- or bi-periodic gratings with a maximum versatility : complex shaped patterns, with anisotropic and graded index material, under oblique incidence and arbitrary polarization. In order to validate our method, we illustrate an example of a four layer dielectric slab, and compare the results with a specific method that we have called *tetrachotomy*, which gives us numerically the poles of the reflection coefficient (which corresponds to the eigenfrequencies of the structure). To illustrate our method, we show the eigenvalues of one- and two-dimensional gratings.

Keywords: resonances, eigenmode analysis, diffraction gratings, finite element method

1. INTRODUCTION

The field of application of diffraction gratings has been extended over the past decades. They are commonly used in various industrial and scientific domains, such as integrated optics, acousto- optics or spectroscopy.[1] For instance, they proved to be particularly efficient as anti-reflective surfaces,[2] beam shapers,[3] waveguide couplers[4] or spectral filters.[5] More than a dozen of numerical methods have already been developed as an answer to this strong need of conceiving and optimizing gratings : (Rigorous Coupled Wave Analysis (RCWA[6]), also known as the Fourier Modal method (FMM[7]), the Chandezon (C) method,[8] differential method,[9] integral method,[10] the Finite-Difference Time-Domain method (FDTD[11]), the method of variation of boundaries...[12]
For spectral filtering applications, one should determine the line shape of the transmission or reflection spectra in order to fit the required features. To avoid the calculation of diffracted efficiencies for a wide range of wavelengths, resonances of the structures should be found. This can be done by searching for complex eigenfrequencies : the real parts correspond to the resonant frequencies and the imaginary parts are related to the damping factors.
This paper is devoted to the study of resonances in different structures by solving an eigenvalue problem with a FEM. It is validated by an independent method that we have called *tetrachotomy* on an example of a four layer dielectric slab. Then the eigenproblem solved by a FEM is applied to one- and two-dimensional gratings. The originality of our approach is that it works irrespective to the geometry and material properties.

2. SET UP OF THE PROBLEM

We denote by $\mathbf{x}$, $\mathbf{y}$ and $\mathbf{z}$ the unit vectors of an orthogonal coordinate system $Oxyz$. We deal with time-harmonic fields, so that the electric and magnetic fields are represented by complex vector fields $\mathbf{E}$ and $\mathbf{H}$ with a time-dependence in $\exp(-i\omega t)$.

We deal with stacks of different layers that may be periodically structured. The materials in this paper are assumed to be isotropic and their optical behaviour is characterized by their relative permittivity ϵ_r and relative permeability μ_r. Note that these scalar fields can be complex-valued, allowing the study of lossy materials, and can vary spatially continuously or discontinuously (graded or step index structures). The domain Ω under study can be divided into several sub-domains, as indicated in Fig. 1 :

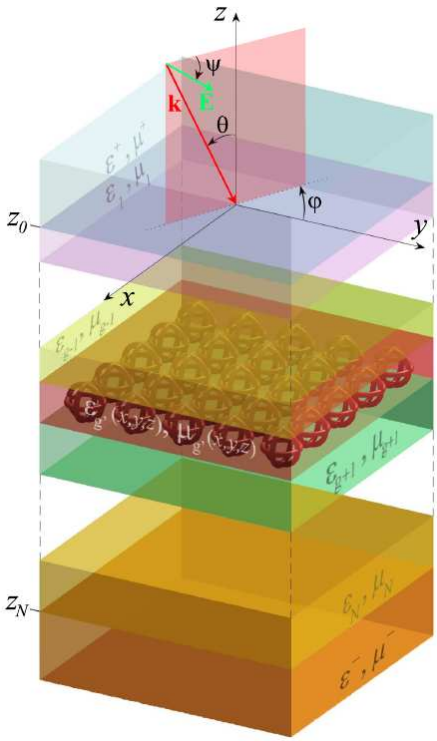

FIGURE 1. Set up of the problem and notations.

- *The superstratum* ($z > z_0$) which is supposed to be homogeneous, isotropic and lossless and characterized solely by its relative permittivity ϵ^+ and its relative permeability μ^+ and we denote $k^+ := k_0\sqrt{\epsilon^+\mu^+}$, where $k_0 := \omega/c$.
- *The multilayered stack* ($z_0 < z < z_N$) composed of N layers which are supposed to be homogeneous and isotropic and therefore characterized by their relative permittivity ϵ_n and their relative permeability μ_n and we denote $k_n := k_0\sqrt{\epsilon_n\mu_n}$
- *The substratum* ($z < z_N$) which is supposed to be homogeneous and isotropic and therefore characterized by its relative permittivity ϵ^+ and its relative permeability μ^- and we denote $k^- := k_0\sqrt{\epsilon^-\mu^-}$
- *The groove region* ($z_{g-1} < z < z_g$) which is embedded in the layer numbered g of the domain under study, which can be heterogeneous and then characterised by the scalar fields $\epsilon_g(x, y, z)$ and $\mu_g(x, y, z)$. The periodicity of the grooves along Ox (resp. Oy) is denoted d_x (resp. d_y).

The grating is illuminated by an incident plane wave of wave vector defined by the angles θ and ϕ : $\mathbf{k}^+ = k^+(\sin\theta\cos\phi, \sin\theta\sin\phi, \cos\theta)^T = (\alpha, \beta, \gamma)^T$. Its electric field $\mathbf{E^0}$ is linearly polarized along the direction defined by the unit vector $\mathbf{A^0}$: $\mathbf{E^0} = \mathbf{A^0}\exp(i\mathbf{k}^+ \cdot \mathbf{r})$, with $\mathbf{r} = (x, y, z)^T$ and $\mathbf{A^0} = (\cos\psi\cos\theta\cos\phi - \sin\psi\sin\phi, \cos\psi\cos\theta\sin\phi + \sin\psi\cos\phi, -\cos\psi\sin\theta)^T$. The problem of diffraction is to find Maxwell's equation solutions in harmonic regime *i.e.* to find the unique solution $\mathbf{E}$ of :

$$-\mathbf{curl}(\mu_r^{-1}\mathbf{curl}\ \mathbf{E}) + k_0^2\epsilon_r\mathbf{E} = 0 \tag{1}$$

such that the diffracted field satisfies an Outgoing Wave Condition and where $\mathbf{E}$ is quasi-periodic with respect to x and y coordinates, *i.e.* :

$$\mathbf{E}(\mathbf{r} + \mathbf{d}) = \mathbf{E}(\mathbf{r})\exp(i\mathbf{k}^+ \cdot \mathbf{d}) = \mathbf{E}(\mathbf{r})\exp(i(\alpha d_x + \beta d_y))$$

with $\mathbf{d} = (d_x, d_y, 0)^T$.

A method[13–16] based on the resolution of the diffraction problem defined by Eq.1, and adapted to the FEM, allows us to extract the transmission, reflection, Joule losses and to obtain a global energy balance.

3. DESCRIPTION OF THE METHODS FOR FINDING RESONANCES

Our purpose is to find resonances of the structures under study. To achieve this, we use two independent methods which are explained in this part. We firstly introduce the following eigenvalue problem.

3.1 The eigenvalue problem

The eigenproblem we are dealing with consists in finding the solutions of *source free* Maxwell's equations. We want to find the complex eigenvalues ω_n and the non vanishing fields $\mathbf{E_n}$ which are bi-pseudo-periodic in Ω and such that :

$$\mathcal{M}(\mathbf{E_n}) := c^2\epsilon_r^{-1}\mathbf{curl}(\mu_r^{-1}\mathbf{curl}\ \mathbf{E_n}) = \omega_n^2\mathbf{E_n}\ . \tag{2}$$

It is of importance to note that the eigenvalues ω_n are generally complex valued and are therefore denoted $\omega_n = \omega_n' + i\omega_n''$ *even if the operator of Maxwell* $\mathcal{M}$ *is formally selfadjoint for lossless materials.* The real part is the resonant frequency and the imaginary part is the damping ratio. The quality factor associated to a resonance is defined by $Q_n := \omega_n'/(2\omega_n'')$. For solving such an eigenproblem, a FEM formulation is used and described thereafter. These eigenvalues may be also considered as poles of the reflection coefficient of the device.[17] The "poles's hunting" is based upon tools of Complex Analysis (called tetrachotomy) and is recalled in the following. Moreover, the double periocity in x and y leads to reduce the eigenproblem to one cell and to use the so-called Bloch decomposition theory and to parametrize the operator at stake by the coefficients of quasi-periodicity α and β which are forced to be real valued despite of the fact that there is no incident plane wave. Thus, the operator of Maxwell ought to have been written $\mathcal{M}_{\alpha,\beta}$. Note that α and β are only a "reminiscence of the incident field " : γ is missing. It is then vain to recover θ and φ thanks to α and β since neither k^+ nor γ are known. It will be given by the eigenvalue ω_n : if ω_n'' is small enough, we can set $k_n^+ \simeq \sqrt{\epsilon^+\mu^+}\omega_n/c$, and deduce the corresponding angles for which a resonance may occur by $\alpha = k_n^+ \sin\theta_n \cos\varphi_n$ and $\beta = \sin\theta_n \sin\varphi_n$. As for the polarization angle ψ the spectrum of the operator $\mathcal{M}_{\alpha,\beta}$ is insufficient : a thorough study of the eigenvectors is essential.

3.2 The FEM formulation

The eigenproblem defined by Eq. 2 is then solved by the FEM, using both PML at the bottom and at the top of the meshed domain and by taking into account the quasi-periodicity conditions on lateral bounds on the same area. Finally, Neumann homogeneous conditions are imposed on the outward edge of each PML. The values of the field on these boundaries gives valuable information on the absorbing efficiency of the PML. Note that the eigenvectors $\mathbf{E_n}$ we are looking for are not of finite energy, but the use of PMLs makes them of finite energy, which is a necessary condition for the weak formulation associated with the FEM.[17–19]
The cell is meshed using 2^{nd} order edge elements. In the numerical examples in the sequel, the maximum element size is set to $\lambda/(N_m\sqrt{\mathfrak{Re}(\epsilon_r)})$, where N_m is an integer (between 6 and 10 is usually a good choice). The final algebraic system is solved using a direct solver (PARDISO).

3.3 The tetrachotomy

As previously said, the eigenvalues of the structure are also the poles of the reflection $r(\omega)$ (or transmission $t(\omega)$) coefficient for the amplitude. Searching for poles is a rather difficult problem, since we do not know *a priori* their number nor their positions in the complex plane. The transmission coefficient can be cast into the following form[17] :

$$t(\omega) = \sum_{n\in\mathbb{N}} \frac{A_n}{\omega - \omega_n} + g(\omega) \tag{3}$$

where the residues $A_n \in \mathbb{C}$ and g is an holomorphic function representing the non-resonant process.
Let Γ be a Jordan curve containing solely the pole ω_m. We define the following complex line integrals I_k for $k = 0, 1, 2$:

$$I_k = \frac{1}{2i\pi}\oint_\Gamma \omega^k t(\omega)\mathrm{d}\omega = \frac{1}{2i\pi}\oint_\Gamma \omega^k \frac{A_m}{\omega - \omega_m}\mathrm{d}\omega \tag{4}$$

since, invoking Cauchy's theorem, the integral of g on a closed loop is null. Applying the residues theorem to $f_k : \omega \mapsto \omega^k \frac{A_m}{\omega - \omega_m}$ leads to :

$$I_k = \mathrm{Res}_{\omega_m} f_k = \lim_{\omega \to \omega_m} (\omega - \omega_m) f_k(\omega) = A_m \omega_m^k$$

Hence, we know the value of $A_m = I_0$ and the pole ω_m is precisely given by :

$$\omega_m = \frac{I_2}{I_1} = \frac{I_1}{I_0} \tag{5}$$

The algorithm of tetrachotomy consists in calculating the poles one by one by dividing sets of rectangular domains (starting with a single initial one) in four isometric parts until we "surround" every pole. We distinguish three cases :

- $I_0 = I_1 = 0$: no pole,
- $\frac{I_2}{I_1} = \frac{I_1}{I_0}$: a single pole given by Eq. 5,
- $\frac{I_2}{I_1} \neq \frac{I_1}{I_0}$: several poles.

The performance of the method is linked to the calculus of the integrals defined by Eq. 4. The details of the method can be found in Ould Agha.[20]

4. VALIDATION : EXAMPLE OF A DIELECTRIC MULTILAYERED STACK

In order to validate the two methods and to compare them in a very simple and academic example, we search for the resonances of a four layer slab, as shown in Fig. 2. The problem is invariant in the (Ox) direction the plane of incidence is $(0xz)$ $(\phi = 0)$. We search for TM polarized fields (the only non-zero component of the magnetic field is H_x), *i.e.* we search for eigenvectors in a subspace such that $\psi = \pi/2$. Under these conditions, the vectorial problem 3.2 reduces to a scalar one. We are looking for resonances at normal incidence ($\theta = 0$), so we set $\beta = 0$ (and hence $\gamma = k^+$). The parameters for the following example are $h_1 = 26\mu$m, $h_2 = 0.5\mu$m, $\epsilon_{air} = 1$, $\epsilon_{Si} = 11.7$, and the relative permittivity[21] of SiO_2 and ZnSe are ploted in Fig. 3 in the far infrared (8-14 µm). In this spectral range, losses can be neglected for ZnSe. Note that we work in the absorption band of SiO_2, both real and imaginary parts of its relative permittivity vary quickly with the wavelength.

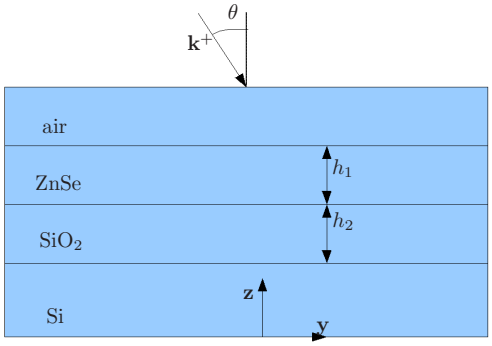

FIGURE 2. Schematic and notations of the slab under study.

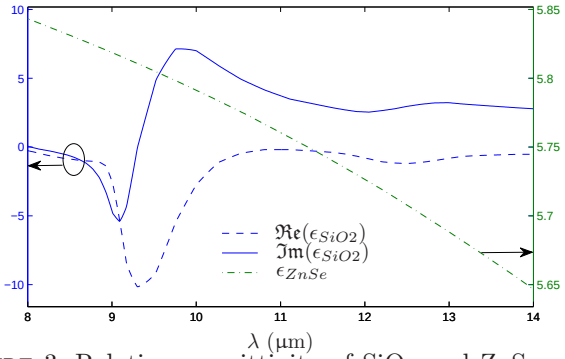

FIGURE 3. Relative permittivity of SiO_2 and ZnSe as a function of the wavelength λ.

Dealing with dispersive materials makes the eigenvalue problem not directly tractable with standards solvers, as the operator of which we want to find the eigenvalues depends itself on the eigenvalue ω via $\epsilon_r(\omega)$. In practice, the permittivity is supposed to be constant : we search N_{eig} eigenvalues $\omega_n^{(1)}$ around the frequency $\omega^{(0)}$ fixed arbitrarily. Then, for $n = 1, 2, \ldots N_{eig}$ we search one eigenvalue $\omega_n^{(2)}$ around $\omega_n^{(1)}$ with updated $\epsilon_r(\omega_n^{(1)})$, and iterate by computing $\omega_n^{(k)}$ until we converge to a fixed point on the value of

$\omega_n^{(k)}$.
Here we obtain the transmission coefficient of the slab by a transfer matrix formalism.[22,23] The numerical scheme used to calculate the integrals defined by Eq. 4 needs to evaluate the transmission coefficient for number of points proportional to the desired precision. The method used to calculate the transmission coefficient needs therefore to be low memory consuming in order to be able to use the tetrachotomy in an efficient way.

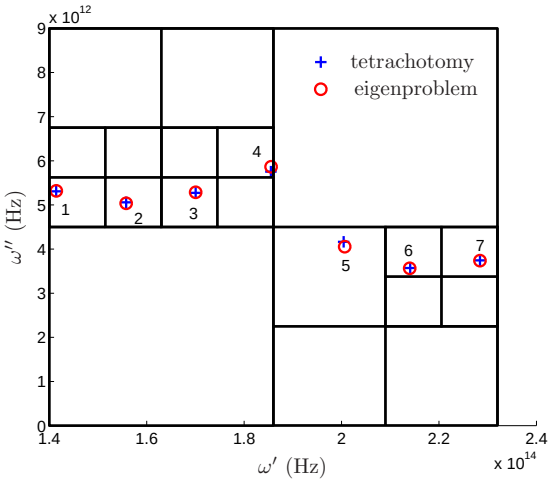

FIGURE 4. Loci of the resonance frequencies in the complex plane for the two methods.

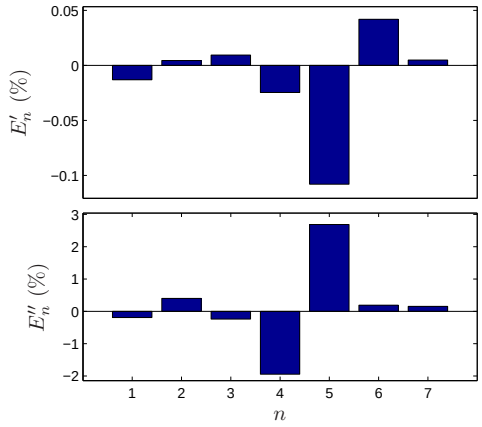

FIGURE 5. Relative difference between the two methods for the n^{th} resonance (top : real parts, bottom : imaginary parts).

Fig. 4 shows the loci in the complex plane of the resonances found by the tetrachotomy and the eigenvalue problem. To compare them, we define the following relative differences :

$$E'_n = \frac{\omega_n^{',tetra} - \omega_n^{',fem}}{\omega_n^{',tetra}} \quad \text{and} \quad E''_n = \frac{\omega_n^{'',tetra} - \omega_n^{'',fem}}{\omega_n^{'',tetra}} \quad \text{for } n = 1, 2, \ldots 7 \tag{6}$$

The two methods are in good agreement as it can be seen in Fig. 5 : the maximum absolute value of the relative difference is of 0.1% for the real parts and of 2.7% for the imaginary parts. Note that this maximum discrepancy occurs for the resonance labelled 7, for which the real part is near 10.6µm. For this wavelength, ϵ_{SiO_2} exhibits a resonant behaviour and corresponds to the resonant frequency of Si-O bound.

Fig. 6 shows the transmittance obtained by a transfer matrix formalism (solid line) and by the FEM (circles). Indeed, we also calculated the transmission by the method described in 2. The two methods are in good agreement, and, as expected, the transmission curves exhibit resonance peaks numbered 1 to 7, corresponding to resonance frequencies depicted in Fig. 4. To illustrate this correspondence, we made a single pole approximation. We suppose that around the pole ω_k, the transmission can be written as :

$$t_n(\omega) = \frac{B_n}{\omega - \omega_n} \tag{7}$$

We can obtain the coefficient $B_n = -i\omega''_n t(\omega'_n)$ by calculating the complex transmittance $t(\omega'_n)$ at the resonance by the FEM. This single poles approximations are plotted in Fig. 6 (dashed curves) : locally around the pole ω_n this is a good approximation, ω'_n defining the peak spectral location and ω''_n defining the peak spectral width.
This example shows that the two methods find similar resonances with a satisfying precision.

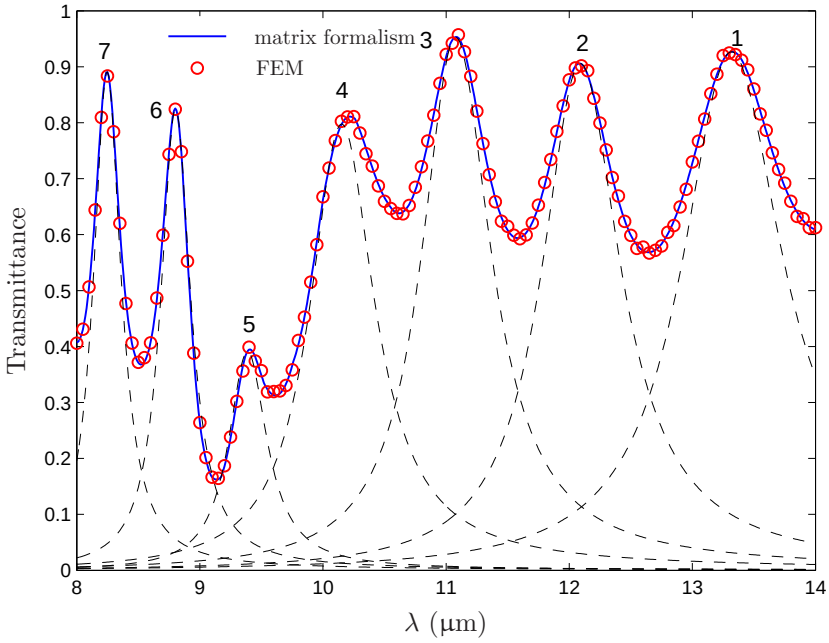

FIGURE 6. Transmittance as a function of the wavelength λ ; dashed lines : single pole approximation.

5. RESONANCE DETERMINATION OF DIFFRACTION GRATINGS

In thist part, we study some examples in the framework of diffraction gratings. The tetrachotomy is not easy to implement for this kind of structures even if closed formulae can be found in some academic examples.[24,25] Moreover, they make assumptions on material characteristics (assuming metals as perfect electric conductors), and geometries (narrow slits), restraining the domain of application of the method. The advantage of the FEM is its complete generality with respect to the geometry and the material properties. In order to study and design gratings with possibly complex shaped diffraction patterns in future works, we now focus on the resolution of the eigenvalue problem using the FEM.

5.1 Example 1

We study mono periodic grating of slits engraved in a metallic film deposited on a dielectric substrate, as shown in Fig. 7. The parameters of the gratings are the period $d = 4\mu$m, the metal thickness $h = 5\mu$m, the slit width $w = 0.7\mu$m. The optical properties are $\epsilon^+ = 1$, $\epsilon^- = 2.25$. The metal used here is chromium which relative permittivity is described by a Drude model[26] :

$$\epsilon_{Cr}(\omega) = \epsilon_\infty - \frac{\omega_p^2}{\omega^2 + i\omega\omega_\tau} \tag{8}$$

with $\epsilon_\infty = 1$, $\omega_p = 36\,650$ cm^{-1}, $\omega_\tau = 440$ cm^{-1}.
We search for resonances at normal incidence ($\theta = 0$), and in TM polarization. The mesh parameter N_M is set to 8.
We find two eigenmodes in the spectral range 8-14 μm (far infrared), the spatial distribution of the real parts of H_x, E_y and E_z are plotted in Fig. 8. The associated eigenfrequencies are ω_1 =283.9+11.4i THz and ω_2 =147.5+22.6i THz.

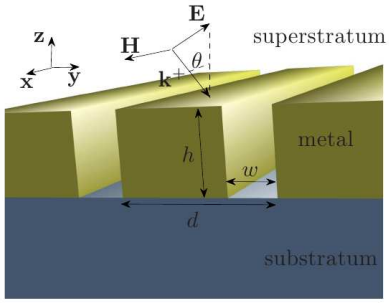

FIGURE 7. Schematic of the grating under study.

n	λ_n	Q_n	λ_n^{fit}	Q_n^{fit}
1	6.63	12.48	6.7	12.5
2	12.77	3.26	12.8	3.3

TABLE 1. Resonance features : λ_n and Q_n obtained by the resolution of the eigenproblem; λ_n^{fit} and Q_n^{fit} extracted from a Gaussian fit (wavelength in µm).

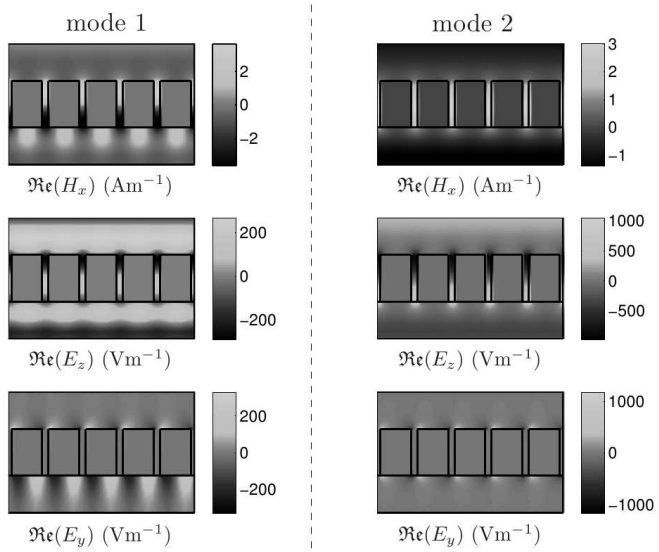

FIGURE 8. Spatial distribution of the real parts of H_x, E_y and E_z for the two eigenmodes.

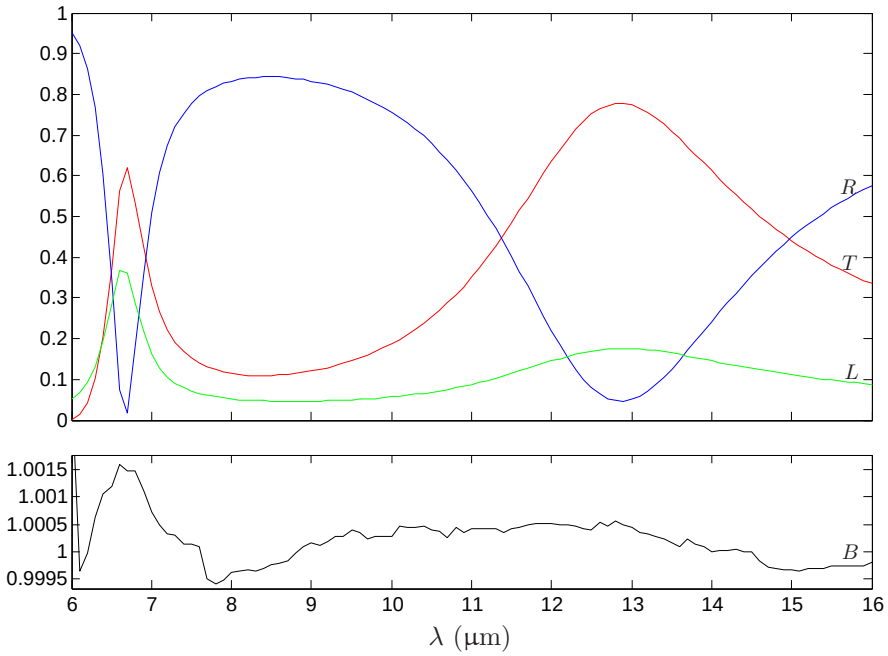

FIGURE 9. Zeroth-order transmission T, zeroth-order reflection R, Joule loss L and energy balance B as a function of the wavelength λ.

To check this result, we solve the diffraction problem with the method mentioned in section 2, for an incident wavelength varying from 8 to 14 µm, and deduce zeroth-order transmission T, zeroth-order reflection R, Joule losses L and energy balance B as a function of the wavelength λ (see Fig. 9). We clearly

observe two transmission peaks. Table 1 shows the two resonances wavelength $\lambda_n = 2\pi c/\omega'_n$ and quality factor $Q_n = \omega'_n/(2\omega''_n)$ calculated by solving the eigenvalue problem, along with λ_n^{fit} and Q_n^{fit} extracted from a Gaussian fit of the transmission curve. For each resonance, both value are in good agreement. The differences are due to the assumption of isolated pole when solving the eigenproblem, whereas there is a coupling between the two modes.

5.2 Example 2

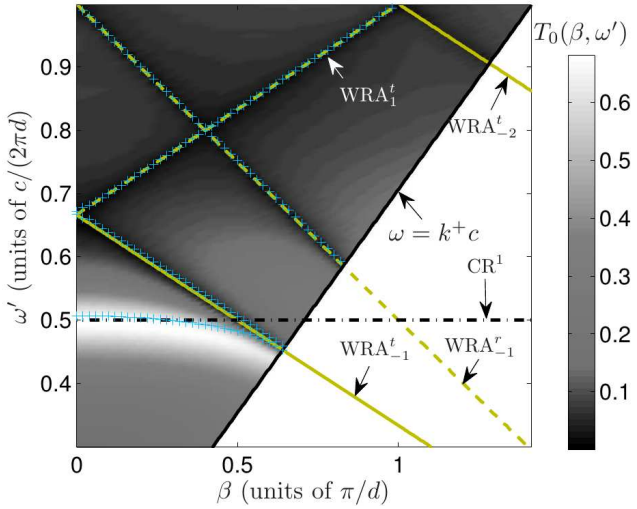

FIGURE 10. Colormap : zeroth-order transmittance $T_0(\beta,\omega')$; + : dispersion diagram $\omega'(\beta)$; — : n^{th} order Wood-Rayleigh anomalies in transmission WRA$_n^t$ (solid) and reflection WRA$_n^r$ (dashed) ; - - - : cavity resonance CR^1.

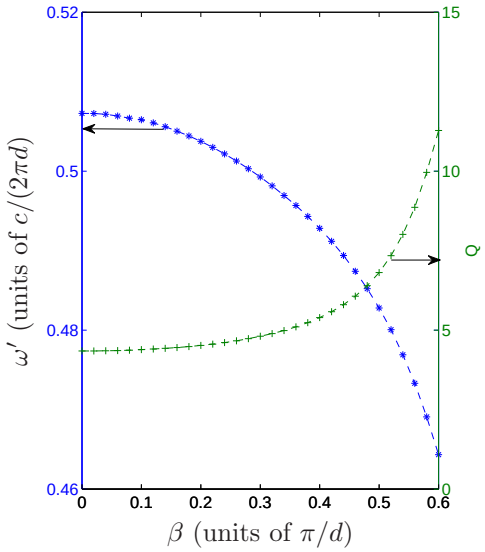

FIGURE 11. Lowest eigenfrequency and associated quality factor as a function of β.

This second example is devoted to illustrate the accuracy of the method for a varying angle of incidence. The structure is the same as in the previous section with $d = 6\mu$m, $h = 4\mu$m and $w = 1\mu$m. We calculated the dispersion diagram $\omega(\beta)$ by searching the eigenvalues for different $\beta \in \mathbb{R}$. We also computed the zeroth-order transmission for varying incident wavelength and angle. We can observe in Fig. 10 that the lowest eigenfrequency follows the transmission maxima when β varies. The others eigenfrequencies appear close to the Wood-Rayleigh anomalies,[27,28] which are due to the appearance/disappearance of a diffraction order and the excitation of surface modes,[29] (in this case surface plasmons). These anomalies occur when the tangential component of the reflected/transmitted plane wave $\beta^{\pm}$ matches the tangential component of the n^{th} diffraction order $\beta_n = \beta_0 + n2\pi/d$, which reads the following condition :

$$\lambda_n^{\pm} = \frac{d}{n}(\sqrt{\epsilon^{\pm}} - \sin\theta) \tag{9}$$

For weak values of β, the spectral position of the lowest resonance frequency is close to the fundamental frequency of a Fabry-Perot like cavity ($\omega_m^{cav} = m\pi c/h$, for $m \in \mathbb{N}^*$) defined by the slit. The associated quality factors are low (see Fig. 11). When β increases, the resonance frequency tends to that of the Wood-Rayleigh anomaly of the -1 transmitted order and the quality factor becomes larger, which means that the resonance peak is sharper, as it can be seen in Fig. 10.

5.3 Example 3

We now study a bi-grating made of a free-standing chromium layer of thickness $h = 800$nm structured with holes of radius r with period $d_x = d_y = d = 8\mu$m, as indicated in Fig. 13. We study the resonances

at normal incidence, as the radius of the holes varies from 1.8 to 2.8 µm. For a given r, we find two eigenvalues, one corresponding to the TE case and the other to the TM case. Because we search for solutions at normal incidence and due to the symmetry of the holes by rotation of $\pi/2$ around the z axis, the eigenvalues corresponding to the two polarization cases are degenerated.[30] Fig. 12 shows that as r increases the resonance peak moves to higher wavelengths and broadens (Q^r decreases). The diffraction problem was solved in TM polarization, for incident wavelengths in the range 7-14 µm, for $r = 2$ µm and $r = 2.5$ µm. We plotted the zeroth-order transmittance $T_{0,0}$ as a function of the wavelength for the two cases in Fig. 14, and extract the features of the resonant peak. As expected by the results of the eigenfrequency analysis, the transmission maximum occurs at $\lambda \simeq 8.4$µm with a quality factor $Q \simeq 13$ for $r = 2$µm, and at $\lambda \simeq 8.7$µm with a quality factor $Q \simeq 5$ for $r = 2.5$µm.

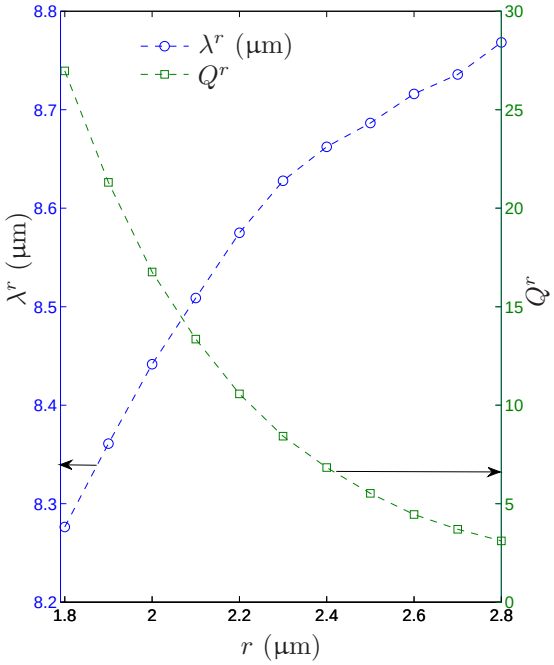

FIGURE 12. Resonance features λ^r and Q^r as a function of the hole radius r.

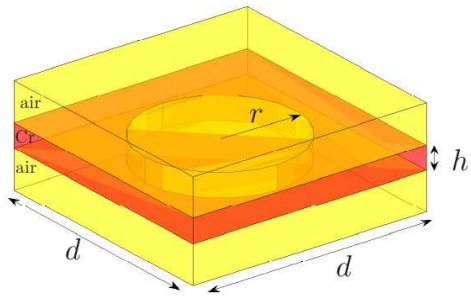

FIGURE 13. Schematic of the hole array under study.

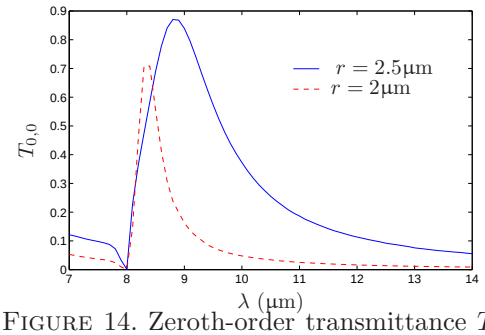

FIGURE 14. Zeroth-order transmittance $T_{0,0}$ as a function of the wavelength for $r = 2$ µm and $r = 2.5$ µm.

6. CONCLUSION

We developed a method to study the resonances in microstructured devices by the FEM. The principles exposed here are independent of the geometry of the diffraction patterns or the number of structured layers.

We validated this method with an example of a four layer slab which transmission features are easily obtained. We then show the eigenvalues of a one dimensional grating of metallic slits deposited on a dielectric substrate, and study their modification with the angle of incidence. Finally we study the resonances of a crossed grating of circular apertures, and study the way they vary with the radius of the holes.

The main advantage of this method is its complete generality with respect to the studied geometries and the material properties, making the method very flexible and adapted to fabrication processes

requirements. Instead of solving the diffraction problem for a whole spectral range to obtain the transmittance, we search for the intimate features of the structures : their eigenmodes and eigenvalues. A resonance is entirely characterized by one point in the complex plane, making parametric studies, design and optimisation easier to realize. Nowadays, the efficiency of the numerical algorithms for sparse matrix algebra together with the available power of computers and the fact that the problem reduces to a basic cell with a size of a small number of wavelengths make the 3D problem very tractable as proved here.

Furthermore, this case can be easily extended to the case of a crossed grating embedded in a multilayered dielectric stack. The generalization to the case of an arbitrary anisotropic diffractive object is straightforward.

REFERENCES

[1] Kikuta, H., Toyota, H., and Yu, W., "Optical elements with subwavelength structured surfaces," *Optical Review* **10**, 63–73 (2003).

[2] Glytsis, E. N. and Gaylord, T. K., "High-spatial-frequency binary and multilevel stairstep gratings : polarization-selective mirrors and broadband antireflection surfaces," *Appl. Opt.* **31**(22), 4459–4470 (1992).

[3] Veldkamp, W. B., "Laser beam profile shaping with binary diffraction gratings," *Optics Communications* **38**(5-6), 381 – 386 (1981).

[4] Schultz, S. M., Glytsis, E. N., and Gaylord, T. K., "Design of a high-efficiency volume grating coupler for line focusing," *Appl. Opt.* **37**(12), 2278–2287 (1998).

[5] Knop, K., "Diffraction gratings for color filtering in the zero diffraction order," *Appl. Opt.* **17**(22), 3598–3603 (1978).

[6] Schuster, T., Ruoff, J., Kerwien, N., Rafler, S., and Osten, W., "Normal vector method for convergence improvement using the RCWA for crossed gratings," *J. Opt. Soc. Am. A* **24**(9), 2880–2890 (2007).

[7] Li, L., "New formulation of the Fourier modal method for crossed surface-relief gratings," *J. Opt. Soc. Am. A* **14**(10), 2758–2767 (1997).

[8] Derrick, G., McPhedran, R., Maystre, D., and Nevière, M., "Crossed gratings : A theory and its applications," *Applied Physics A : Materials Science ; Processing* **18**, 39–52 (1979).

[9] Maystre, D. and Neviere, M., "Electromagnetic theory of crossed gratings," *Journal of Optics* **9**(5), 301 (1978).

[10] Maystre, D., "A new general integral theory for dielectric coated gratings," *J. Opt. Soc. Am.* **68**(4), 490–495 (1978).

[11] Yee, K. S., "Numerical solution of initial boundary value problems involving Maxwell's equations in isotropic media," *IEEE Trans. Antennas and Propagation* , 302–307 (1966).

[12] Bruno, O. P. and Reitich, F., "Numerical solution of diffraction problems : a method of variation of boundaries. III. Doubly periodic gratings," *J. Opt. Soc. Am. A* **10**(12), 2551– 2562 (1993).

[13] Demésy, G., Zolla, F., Nicolet, A., Commandré, M., and Fossati, C., "The finite element method as applied tothe diffraction by an anisotropic grating," *Opt. Express* **15**(26), 18089–18102 (2007).

[14] Demésy, G., Zolla, F., Nicolet, A., and Commandré, M., "Versatile full-vectorial finite element model for crossed gratings," *Opt. Lett.* **34**(14), 2216–2218 (2009).

[15] Demésy, G., Zolla, F., Nicolet, A., and Commandré, M., "All-purpose finite element formulation for arbitrarily shaped crossed-gratings embedded in a multilayered stack," *J. Opt. Soc. Am. A* **27**(4), 878–889 (2010).

[16] Demésy, G., Zolla, F., Nicolet, A., and Commandré, M., "An all-purpose three-dimensional finite element model for crossed-gratings," in [*Proceedings SPIE*], **7353**, 73530G (2009).

[17] F. Zolla, G. Renversez, A. Nicolet, B. Kuhlmey, S. Guenneau and D. Felbacq, [*Foundations of photonic crystal fibres (second edition)*], Imperial College Press (2012).

[18] Nicolet, A., Zolla, F., Ould Agha, Y., and Guenneau, S., "Leaky modes in twisted microstructured optical fibers," *Waves in Random and Complex Media* (17), 559 (2007).

[19] Ould Agha, Y., Zolla, F., Nicolet, A., and Guenneau, S., "On the use of PML for the computation of leaky modes : an application to gradient index MOF," *COMPEL* **27**(1), 95–109 (2008).

[20] Ould Agha, Y., *Transformations géométriques réelles et complexes : application à la recherche de modes à pertes dans des fibres optiques microstructurées*, PhD thesis, Université Paul Cézanne - Aix-Marseille III (2007).
[21] Palik, E. D., [*Handbook of optical constants of solids*], Academic Press (1991).
[22] Macleod, H., [*Thin-film optical filters (3rd edition)*], Institute of Physics Pub. (2001).
[23] Petit, R., [*Ondes électromagnétiques en radioélectricité et en optique*], Masson (1993).
[24] Kukhlevsky, S., Mechler, M., Samek, O., and Janssens, K., "Analytical model of the enhanced light transmission through subwavelength metal slits : Green's function formalism versus Rayleigh's expansion," *Applied Physics B : Lasers and Optics* **84**, 19–24 (2006).
[25] Yang, R., Rodriguez-Berral, R., Medina, F., and Hao, Y., "Analytical model for the transmission of electromagnetic waves through arrays of slits in perfect conductors and lossy metal screens," *Journal of Applied Physics* **109**(10), 103107 (2011).
[26] Fouad, S. S., Ammar, A. H., and El-Fazary, M. H., "A New Approach to the Correlation of the Electrical Properties with Interband and Intraband Transitions of Thin Cr Films," *physica status solidi (b)* **187**(1), 99–108 (1995).
[27] Wood., R., "On a remarkable case of uneven distribution of light in a diffraction grating spectrum," *Proceedings of the Physical Society of London* (18), 269–275 (1902).
[28] Rayleigh, L., "Note on the remarkable case of diffraction spectra described by Prof. Wood," *Philos. Mag.* (14), 60–65 (1907).
[29] Hessel, A. and Oliner, A. A., "A New Theory of Wood's Anomalies on Optical Gratings," *Appl. Opt.* **4**(10), 1275–1297 (1965).
[30] Fehrembach, A.-L. and Sentenac, A., "Study of waveguide gratings eigenmodes for unpolarized filtering applications," *Journal of the Optical Society of America A* **20**, 481–488 (2003).